THE JOURNAL OF PHYSICAL CHEMISTRY LETTERS
A JOURNAL OF THE AMERICAN CHEMICAL SOCIETY

pubs.acs.org/JPCL Letter

Vanadium Cluster Neutrals Reacting with Water: Superatomic Features and Hydrogen Evolution in a Fishing Mode

Hanyu Zhang,[#] Mingzheng Zhang,[#] Yuhan Jia, Lijun Geng, Baoqi Yin, Shunning Li, Zhixun Luo,* and Feng Pan*

Cite This: *J. Phys. Chem. Lett.* 2021, 12, 1593−1600 Read Online

ABSTRACT: Hydrogen evolution reaction (HER) is known as the heart of various energy storage and conversation systems of renewable energy sources. Here we observe the cluster reactions of a light transition metal, vanadium, with water in a gas-phase flow tube reactor. While HER products of V_1 and V_2 were not observed, the effective HER of water on neutral V_n ($n \geq 3$) clusters reveals reasonable and size-dependent reactivity of the vanadium clusters. Superatomic features and reaction dynamics of V_{10}, V_{13}, and V_{16} are highlighted. Among the three typical superatoms, V_{10} and V_{16} exhibit an abnormal superatomic orbital energy level order, 1S|2S|1P|1D..., where the energy-reduced 2S orbital helps to accommodate the geometric structure and hence reinforce the cluster stability. In comparison, V_{13} bears a less symmetrical structure and reacts readily with water, allowing for recombination of a hydroxyl atom with an adsorbed hydrogen atom, akin to a fishing-mode HER process. The joint experimental and theoretical study on neutral V_n clusters clarifies the availability of superatom chemistry for transition metals and appeals further development of cluster theory based on electronic cloud/orbital analysis instead of simply counting the valence electrons. Also, we provide insights into the HER mechanism of metal clusters and propose a strategy to design new materials for portable fuel cells of hydrogen energy.

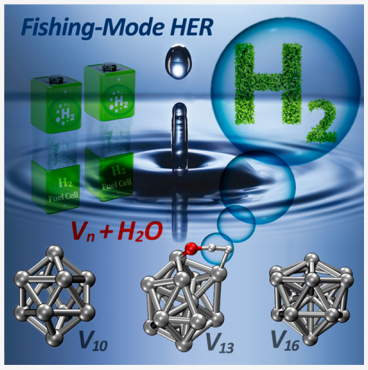

Advances in exploring nanocatalysts have unveiled that transition metal clusters having a particle size of less than 2 nm exhibit highly active catalysts for numerous chemical procedures. Owing to the specific electronic and geometric structures, chosen metal clusters could exhibit higher stability or reactivity as compared to clusters of other sizes.[1−4] On the basis of the near free electron gas (NFEG) theory of metals and the jellium model,[5−7] highly degenerated electronic states can be attained for spherical clusters within the symmetric potential function,[8−10] on which a referable criterion to predict cluster stability/reactivity has been established by solving average central potentials to obtain magic numbers. For instance, the spherically symmetric harmonic oscillator predicts the magic number of electron counts at 2, 8, 20, 40, 58, ...; the Clemenger−Nilsson model allows for ellipsoidal distortion or harmonic oscillator distortion,[7] enabling us to rationalize stable clusters with altered midshells from prolate to oblate and a variety of nuclei and various valence electron counts at 2, 8, 18, 20, 34, 40, 58, 70, etc.[6,7] These magic numbers are also obtained by solving the Kohn−Sham equations with a square well function or a Woods−Saxon potential well function.[5,11] While the jellium model (including Clemenger−Nilsson distortion) on valence electrons has been successfully applied to predict magic numbers and explain the cluster stability of various metals (typically s- and p-blocks of the periodic table of elements as well as coinage metals), there is a difficulty to estimate the valence electron counts for transition metal clusters because of the complexity of localized d and f electrons.

With the development of cluster science and superatom chemistry,[8−10,12] research interest in finding stable metal clusters is not limited to magic numbers but includes the exploration of clusters to mimic the chemical behavior of a certain atom or a family of elements in the periodic table. It has been recognized that radial extension of the outermost d-electrons could give rise to effectively delocalized electronic configuration across a superatom cluster of transition metals.[13−15] In this regard, superatomic features could be better presented by orbital and graphical illustration instead of simply counting the valence electrons. In the pursuit to find other superatom clusters, it is also important to unveil the difference between an ion−molecule reaction and superatom cluster reaction, to understand how transition metal clusters are also subject to the superatom theory thus full insights into nanocatalysis and surface chemistry.

Received: December 26, 2020
Accepted: January 31, 2021
Published: February 5, 2021

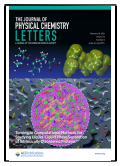

https://dx.doi.org/10.1021/acs.jpclett.0c03809
J. Phys. Chem. Lett. 2021, 12, 1593−1600

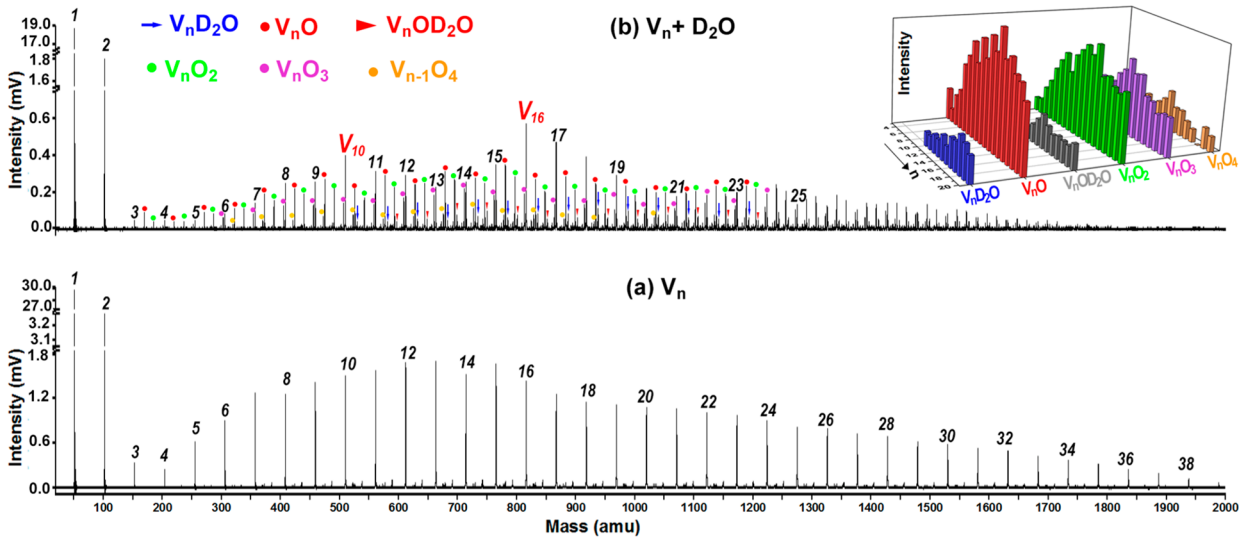

Figure 1. Mass spectra of neutral V_n clusters (a) and after reacting with D_2O (b), with the partial pressures of D_2O vapor in the reaction tube at ∼60 mPa.

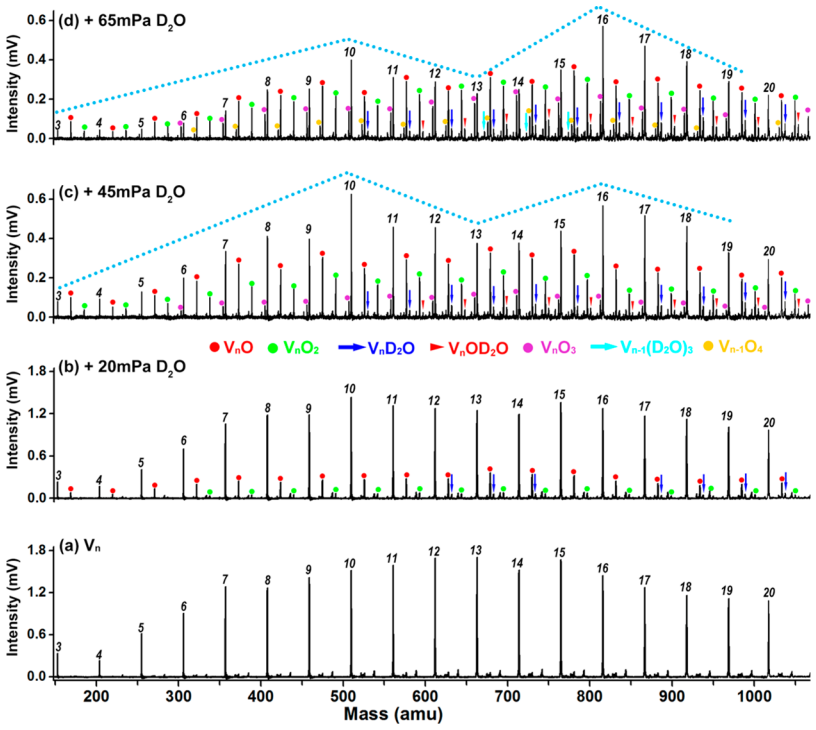

Figure 2. Mass spectra of (a) neutral V_n (n = 1−20) clusters and (b)−(d) V_n reacting with different amounts of D_2O with the partial pressures of D_2O vapor in the reaction tube at ∼20, ∼45, and ∼65 mPa.

Metal cluster stability and reactivity are often determined by gas-phase reactions.[3,16] For example, the reactivity of Al cluster anions with water demonstrated that complementary active sites account for the size-selective reactivity, unveiling dependence on geometric rather than electronic shell structure.[2] Also, extensive studies have revealed the diverse reactivities of transition metal ions and clusters in a variety of conditions,[17−35] motivated by the application potentials in catalysis,[36] battery cathodes, and magnetic materials.[37,38] Among them, the studies on the size-dependent reactivity of vanadium clusters with CO, NO, O_2, D_2, N_2, C_xH_x, alcohols, and many other species have been conducted,[29−35,39] allowing us to quantitatively estimate the reaction probability and catalytic behavior. In particular, several studies have revealed the geometric structures, electronic properties, and kinetics involved in the novel coordination chemistry of vanadium cations with water,[17−25] as well as electronic properties of hydrated V_n clusters.[40] Recently, we studied the reactions of ionic vanadium clusters and found significant H_2 release from single H_2O molecules in reacting with cationic V_n^+,[41] revealing decisive advantages of vanadium clusters (rather than single atoms) for hydrogen evolution reaction (HER) from water. On this basis, further insights into HER from neutral metal clusters are essentially significant to clarify the efficient reactions of clusters versus single atoms and to design strategy for new materials of hydrogen energy used for portable fuel cells.

https://dx.doi.org/10.1021/acs.jpclett.0c03809
J. Phys. Chem. Lett. 2021, 12, 1593−1600

However, the fact that the V−V metal bond is much weaker than the V−O bond makes it a challenge to prepare uncontaminated pure vanadium metal clusters. In particular, the likely fragmentation of neutral clusters caused by the multiphoton ionization process could impede the acquisition of intact information. Recently, we have developed an integrated instrument of reflection a time-of-flight mass spectrometer (Re-TOFMS) with an ultrafast deep-ultraviolet (DUV) laser for photoionization. The DUV laser (177.3 nm) has a short pulse duration (15 ps) and appropriate pulse energy (∼20 μJ),[42−44] which happens to be applicable for highly efficient and low-fragment photoionization of the neutral vanadium clusters and their hydrates. Taking advantage of the DUV laser ionization and our experiences in preparing metal clusters, we have been able to observe the well-resolved mass distribution of neutral vanadium clusters V_n (n = 1−40), and here we have studied the gas-phase reactions with a few chemicals including N_2, CO_2, and D_2O in the flow-tube reactor (the etching reaction with O_2 reported in the previous study[44]). Interestingly, the reactions with water clearly screen out reasonable stability of superatomic V_{10} and V_{16} with a contrast to the relatively reactive V_{13} cluster, which prompts the hydrogen evolution from water. With an emphasis on the typical superatom−molecule reaction "V_{13} + H_2O" versus atom−molecule reaction "V_1 + H_2O", we illustrate the reaction kinetics within a fishing-like mode, that is, a terminal hydrogen interacting with an adsorbed hydrogen atom for H_2 release.

Reactions between deuterium water and neutral vanadium clusters comprising 1−40 atoms (Figure 1) were observed under multicollisional conditions in a fast-flow tube reactor. When water was introduced into the tube reactor, a variety of reaction products were observed that we have assigned as V_nD_2O, V_nO, V_nOD_2O, V_nO_2, $V_n(D_2O)_3$, V_nO_3, and V_nO_4 series with varying intensities. Among them, the series of V_nOD_2O and V_nO_2 dominate the mass distributions of the observed products, indicating two water molecules are favored for hydrogen release on the neutral vanadium clusters ($n \geq 3$). It is seen that the large ones (e.g., $n \geq 10$) allow for adducts of a V_n cluster with water, whereas the small ones readily react along with hydrogen release. This is different from the previous studies of aluminum cluster anions in reaction with water where less HER products were observed for the small ones.[2,45] The minor difference of reactivity for the clusters of similar sizes suggests an essential distinction in electronic and geometric structures.

V_3 is found to be the smallest cluster that reacts with water to produce hydrogen among the studied clusters, shedding light on the importance of the multisites cooperative effect.[12,46] Figure 2 presents the mass spectra of the neutral vanadium clusters V_n with a size of n = 3−20 in the presence of different amounts of deuterated water (∼2% D_2O in He) in the flow-tube reactor (full-scale spectra for n = 1−38 are given in Figure S1). The partial pressures of D_2O vapor in the reaction tube are controlled at ∼20, ∼45, and ∼65 mPa, corresponding to mass spectra in Figure 2b−d. With an increasing concentration of D_2O, the mass abundances of dehydrogenation products gradually increase, giving rise to V_nO_3 and V_nO_4 series, indicative of multiple water molecule reactions in sequence. The discrimination of V_nOD_2O suggests that the hydrogen release from the water via an adsorption-dissociation process. It is worth noting the size dependence of V_n clusters in reacting with water molecules. Interestingly, V_{13} is largely consumed in the presence of relatively more water vapor, while both V_{10} and V_{16} find prominent intensities in the mass distributions. Repeated experiments of V_n reacting with heavy-oxygen water ($H_2{}^{18}O$) bring forth the same conclusion of size dependence (Figure S2) and verify the oxygen is from the water reactant instead of trace amounts of oxygen contamination (oxygen-16) in the vacuum chamber. Comparison experiments on pure helium gas were also conducted, showing the altered mass distribution is not resulted from increased He gas collisions (Figure S3a). In addition, we have also studied the reactions of V_n clusters with N_2 and CO_2 (Figures S3 and S4) and found the reaction with water shows the most conspicuous size dependence among these studies.

In order to clearly display the size-dependent stability and reactivity of V_n clusters with water, Figure 3 plots the normalized relative rate constants. Considering the incomplete depletion of the nascent vanadium clusters, the HER channels for V_n to react with a different number of H_2O molecules in producing a series of products can be written as an integral chemical equation pertaining to pseudo-first-order reactions,

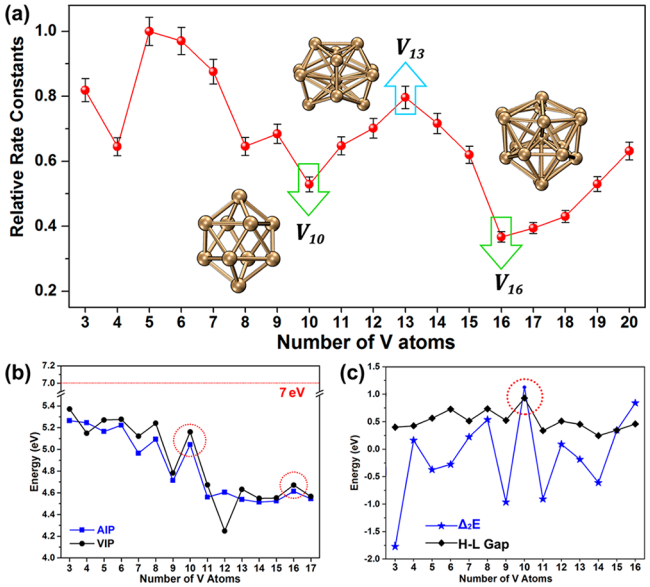

Figure 3. (a) Normalized relative rate constants k_n^{rel}, n = 3−20. The insets show the lowest-energy structures of V_n clusters optimized at BPW91/TZVP level of theory. (b) Adiabatic ionization potentials (AIP) and vertical ionization potentials (VIP) of the neutral V_n (n = 3−17) clusters. (c) Plots of the second-order differences in binding energies (Δ_2E, blue line) and HOMO−LUMO gaps (H−L gap, black line) of V_n clusters.

$$V_n + m(H_2O) \rightarrow V_nO_x(H_2O)_{m-x} + xH_2 \qquad (m \geq 3) \tag{1}$$

On this basis, we estimated the pseudo-first-order rate constants (k_n) simply by the following equation,[41,44]

$$k_n = -\ln(A/A_0) = -\ln(I_{V_n'}/I_{V_n^0})/(\rho \cdot t) \tag{2}$$

and identified the normalized relative rate constants k_n^{rel} as

$$k_n^{rel} = k_n/k_5 \qquad (n = 3 - 20) \tag{3}$$

in which $I_{V_n^0}$ and $I_{V_n'}$ are the intensities of V_n before and after the reaction. t is the effective residence time in the reactor (∼60 μs) and ρ is the molecule number density. As is plotted

https://dx.doi.org/10.1021/acs.jpclett.0c03809
J. Phys. Chem. Lett. 2021, 12, 1593−1600

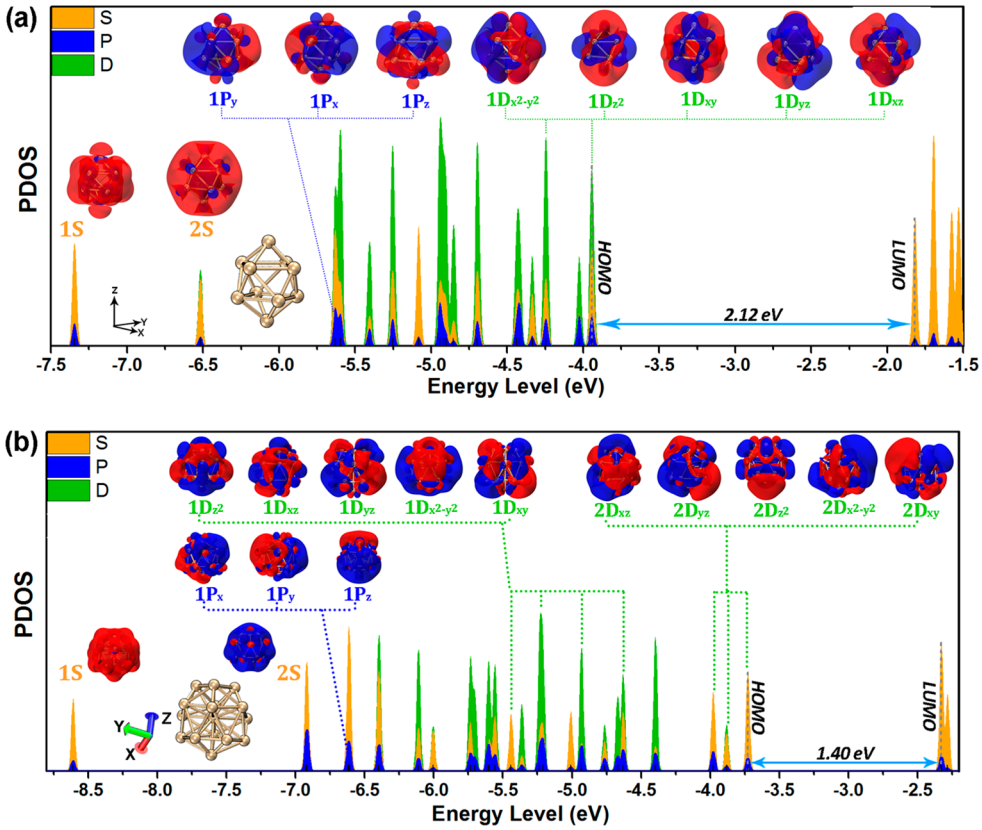

Figure 4. (a, b) Partial density of states (PDOS) and selected canonical molecular orbitals (CMOs) of neutral V_{10} and V_{16} clusters, calculated at the B3LYP/TZVP level. The HOMO−LUMO gaps are given in eV. The orange, blue, and green curves indicate the PDOS of S, P, and D shell types, respectively.

in Figure 3a, the k_n^{rel} values of V_n ($3 \leq n \leq 20$) illustrate size-dependent reaction rates with local minimum values at $n = 10$ and 16 and local maxima at $n = 5$ and 13. The smaller reaction rates of V_{10} and V_{16} in such chemicals suggest their relative inertness pertaining to higher stability.

We have performed comprehensive DFT calculations to investigate the inner determinants of the size-dependent reactivity and reveal the hydrogen evolution mechanism. Global research of the neutral vanadium clusters was conducted on a basis of USPEX[47] combined with VASP[48] (for details see Figures S5−S7), and the energy-minima structures of V_n clusters ($n = 1$−16) were further optimized at the BPW91[49,50]/TZVP[51] level of theory using the Gaussian 09 program package.[52] Considering the diversity of spin electrons of the small transition metal clusters,[53−55] we have also checked the magnetic moments and the electronic states of the lowest energy structures of the V_n clusters (Figures S8 and S9). As a result, a closed-shell bicapped square antiprism,[40] with the point group D_4, was found to be the ground state of V_{10}. Also, a singlet spherical structure with C_{3v} symmetry was found for V_{16}.[56] The lowest-energy structure of V_{13} has a distorted icosahedron structure with a doublet spin state. Figures 3b presents the calculated adiabatic ionization potential (AIP) and vertical ionization potential (VIP) of the neutral V_n ($n = 3$−17) clusters. Also calculated, are the second-order differences in binding energies, Δ_2E, defined by $\Delta_2E = E(V_{n+1}) + E(V_{n-1}) - 2E(V_n)$, and the HOMO−LUMO gaps of these neutral V_n clusters. As is shown in Figure 3c, all the AIP and VIP values are less than 7 eV (the single-photon energy of the DUV laser), among which V_{10} and V_{16} bear relatively larger values than that of the neighboring V_n clusters. This is consistent with the previous experimental results that V_{10} bears the largest ionization energies (IE)[57] among V_n ($n = 3$−13) clusters. As for the HOMO−LUMO gaps, V_{10} also possesses the largest value among the studied clusters, as well as the largest dissociation energies determined by the previous study.[40] In all, the energetics analysis indicates that V_{10} and V_{16} could be the two most stable clusters in the V_n ($n = 3$−16) series.

It is commonly understood that a comprehensive picture to justify the stability of a metal cluster could involve both geometric structure and electronic configuration as well as the resulted energetics.[12] Having determined the cluster structures and energetics, we then calculated the partial density of states (PDOS) and checked the canonical molecular orbitals (CMOs) to provide further insights into the electronic configuration of these vanadium clusters. The results of V_{10} and V_{16} clusters are shown in Figure 4 (more information in Figures S13 and S14). It is remarkable that their degenerate electron shells are akin to atomic orbitals, corresponding to superatomic S, P, and D orbital characteristics. Such an orbital feature provides robust evidence of the superatomic nature of such transition metal clusters. This is consistent with the previous studies that the transition metals could significantly contribute valence electrons to the global electronic structure. What is intriguing is that superatomic orbitals of both V_{10} and V_{16} display neighboring 1S and 2S inner shell structure. The dual superatomic S orbital encompassing the whole cluster could bring forth radial extension of the global shell structure and thus accommodation of the spherical geometry analogous

https://dx.doi.org/10.1021/acs.jpclett.0c03809
J. Phys. Chem. Lett. 2021, 12, 1593−1600

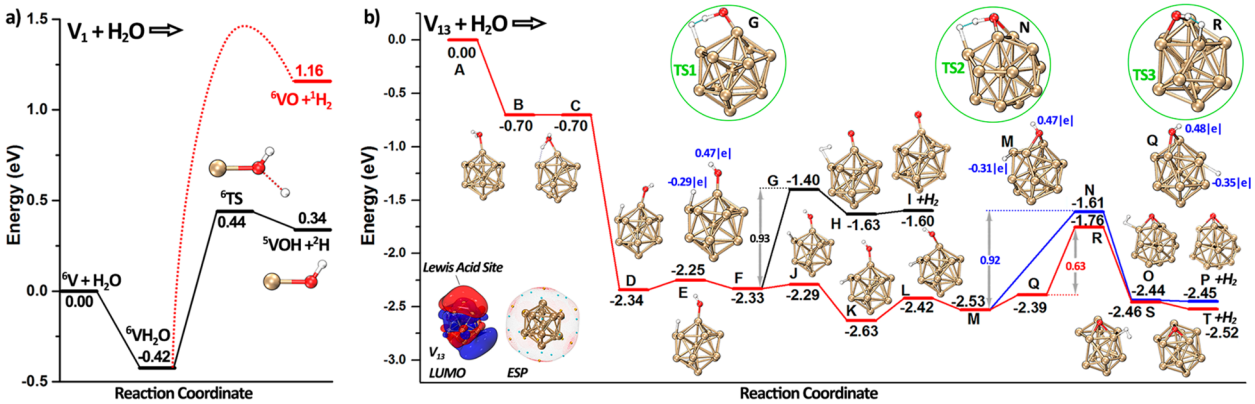

Figure 5. Reaction pathways for "$V_1 + H_2O$" (a) and "$V_{13} + H_2O$" (b). The energy values are relative to the entrance channel, are corrected with zero-point vibration energies, and are given in eV. The marked partial charges on hydrogen atoms of the intermediates ($HV_{13}OH$) are calculated at BPW91/TZVP level of theory using natural bond orbital (NBO) method. Also displayed, are the lowest unoccupied molecular orbital (LUMO) and surface electrostatic potential (ESP), as well as the optimized structures of intermediates and transition states.

to electron shell of atoms. It is reported that the exact exchange in the functional influences the transition metal superatom orbitals,[14,15] but in this case, the functional BPW91 (Figure S14) and B3LYP[58,59] (Figure 4) give the same conclusion that V_{10} and V_{16} own neighboring 1S and 2S orbitals. In addition to the energy-reduced 2S orbital, V_{10} also displays clear superatomic 1P and 1D orbitals, and V_{16} exhibits extra 2D orbitals. Note that the lowest energy structure of V_{13} does not have high symmetry, and $V_{13}H_2O$ bears a large V-water binding energy, a short V−O bond length (a large bond order), and large net electron transfer between the V_{13} moiety and water (Tables S3 and S4, Figure S17).

We then examined the thermodynamic energy changes for all the "$V_n + H_2O$" reactions (Figure S19). It is found that the changes of enthalpy energies ($\Delta_r H_0$, eV) and Gibbs free energies (ΔG, eV) for these reactions exhibit minor odd−even alternation, which is likely due to the variation of unpaired electron spin density (UPSD) distributions (Figure S10) pertaining to altered stability and activity of the V_n clusters. It is amazing that V_5 and V_{13} exhibit larger HER energy release, which is very consistent with the aforementioned experimental observation and also agrees with the previously published study on cationic vanadium cluster reactions.[41] Note that V_5 aims at the critical point of 2D-to-3D structure transition, and V_{13} corresponds to a collapse of the icosahedron structure. Also, we have plotted the reaction coordinates of water with the V_n clusters (n = 1, 2, 3, 10, 13, 16) based on DFT calculations, with a comparison of "$V_1 + H_2O$" versus "$V_{13} + H_2O$" shown in Figure 5. The ground state $^6V_1$ undergoes an endothermic (1.16 eV) hydrogen release process, which is significantly larger than the energy to remove a free hydrogen atom (also endothermic with an insurmountable transition state). While the reaction "$V_2 + H_2O$" is exothermic (Figure S20b), the energy barrier in the rate-determining step is up to 1.51 eV; thus, it is also difficult for hydrogen evolution. This is very consistent with the experimental results of no HER products being observed for V_1 and V_2 in the mass spectra (Figure 1b; also Figures S1 and S2).

The HER energy diagram of "$V_{13} + H_2O$" is provided in Figure 5b. The superatom cluster V_{13} is taken as an example because $V_{13}O$ is the most outstanding product in V_nO series and the 13-atom clusters often correspond to superatom character with a likely closure of geometric shell. It is seen that the lowest energy structure of $V_{13}H_2O$ (step B) undergoes dissociation of the O−H bond in water with a barrierless step toward the transition structure C, and then the hydrogen atom falls to the surface of V_{13}. The other hydrogen atom will rotate to a suitable angle allowing the two hydrogens to face each other (from D to F) by suffering a small barrier of 0.09 eV. Note that the first O−H bond is dissociative and the hydrogen atom can migrate easily on the vanadium cluster surface. Before forming H_2, the oxygen atom may selectively stay on the atop site (black path) or hollow site (red path). For the black pathway where the oxygen atom stays on the atop site, the two hydrogen atoms can attach to each other and form a transition structure G with a single-step energy barrier of 0.93 eV. For the red pathway, the oxygen atom will migrate to the hollow site, allowing the two hydrogen atoms to approach each other and form a transition state N, with a comparable energy barrier of 0.92 eV. Although the barriers of the two pathways are similar, the hollow site product is more stable than that of the atop site, with a large energy difference up to 0.85 eV. In addition, the dissociatively adsorbed H atom could migrate on the vanadium cluster simply by overcoming a small step of energy, enabling for an optimal H_2-recombination transition state with reduced energy barrier of the rate-determining step (0.63 eV vs 0.92 eV). The hydrogen release through recombination of an adsorbed H atom and a hydroxyl hydrogen (i.e., $H_{ad} + H_{hydroxyl} \rightarrow H_2$) goes like a fishing reaction mode driven by electrostatic attraction between the electronegative and electropositive H atoms (see partial charges for detail in the insets of Figure 5b). Such fishing-mode reaction pathways are also addressed for V_3, V_{10}, and V_{16} (Figures S20−22). Essentially, this mechanism differs from the previously established HER mechanism of two water molecules on aluminum cluster anions by recombination of two adsorbed hydrogen atoms (i.e., $H_{ad} + H_{ad} \rightarrow H_2$). For the final V_nO products, the oxygen atoms tend to locate on the triangle surfaces formed by three V atoms.[60]

The HERs of water on neutral vanadium clusters have been studied utilizing a customized reflection time-of-flight mass spectrometer (Re-TOFMS) combined with a homemade 177.3 nm DUV laser for photoionization. We illustrate the stability and superatomic orbital characteristic of V_{10} and V_{16} clusters. Interestingly, the two clusters both display well-delocalized electron density and degenerate electronic shell structure allowing the energy-reduced superatomic 2S orbital to encompass the whole cluster, thus a radial extension of the

https://dx.doi.org/10.1021/acs.jpclett.0c03809
J. Phys. Chem. Lett. 2021, 12, 1593−1600

global shell structure, which is beneficial to electronic accommodation for spherical geometry analogous to atoms. Density functional theory calculation also reveals that V_{10} and V_{16} possess large second-order binding energies and HOMO−LUMO gaps in comparison with other neutral V_n clusters, which accounts for their unique stability. Also, we demonstrate the HER reactivity of such transition metal clusters by taking V_{13} as an example, shedding light on the HER mechanism with a fishing-like transition state.

■ ASSOCIATED CONTENT

Supporting Information

The Supporting Information is available free of charge at https://pubs.acs.org/doi/10.1021/acs.jpclett.0c03809.

Experimental and theoretical methods; Tables S1−S6 of bond dissociation energies, bond distances, binding energies, EDA results, VIE, and atomic charges and electronic configurations; Figures S1−22 of mass spectra, enthalpies and structures, spin densities, electronic affinity, partial charge, orbitals, PDOS, binding energies, total energies, reaction pathways (PDF)

■ AUTHOR INFORMATION

Corresponding Authors

Zhixun Luo − *Beijing National Laboratory of Molecular sciences (BNLMS), State Key Laboratory for Structural Chemistry of Unstable and Stable Species, Institute of Chemistry, Chinese Academy of Sciences, Beijing 100190, P. R. China; University of Chinese Academy of Sciences, Beijing 100049, P. R. China;* orcid.org/0000-0002-5752-1996; Email: zxluo@iccas.ac.cn

Feng Pan − *School of Advanced Materials, Peking University Shenzhen Graduate School, Shenzhen 518055, P. R. China;* orcid.org/0000-0002-8216-1339; Email: panfeng@pkusz.edu.cn

Authors

Hanyu Zhang − *Beijing National Laboratory of Molecular sciences (BNLMS), State Key Laboratory for Structural Chemistry of Unstable and Stable Species, Institute of Chemistry, Chinese Academy of Sciences, Beijing 100190, P. R. China; University of Chinese Academy of Sciences, Beijing 100049, P. R. China;* orcid.org/0000-0002-9745-234X

Mingzheng Zhang − *School of Advanced Materials, Peking University Shenzhen Graduate School, Shenzhen 518055, P. R. China*

Yuhan Jia − *Beijing National Laboratory of Molecular sciences (BNLMS), State Key Laboratory for Structural Chemistry of Unstable and Stable Species, Institute of Chemistry, Chinese Academy of Sciences, Beijing 100190, P. R. China; University of Chinese Academy of Sciences, Beijing 100049, P. R. China*

Lijun Geng − *Beijing National Laboratory of Molecular sciences (BNLMS), State Key Laboratory for Structural Chemistry of Unstable and Stable Species, Institute of Chemistry, Chinese Academy of Sciences, Beijing 100190, P. R. China; University of Chinese Academy of Sciences, Beijing 100049, P. R. China*

Baoqi Yin − *Beijing National Laboratory of Molecular sciences (BNLMS), State Key Laboratory for Structural Chemistry of Unstable and Stable Species, Institute of Chemistry, Chinese Academy of Sciences, Beijing 100190, P. R. China*

Shunning Li − *School of Advanced Materials, Peking University Shenzhen Graduate School, Shenzhen 518055, P. R. China*

Complete contact information is available at: https://pubs.acs.org/10.1021/acs.jpclett.0c03809

Author Contributions

[#]H.Z. and M.Z. contributed equally to this work.

Notes

The authors declare no competing financial interest.

■ ACKNOWLEDGMENTS

Financial support for this work was provided by the National Natural Science Foundation of China (21722308), the National Project Development of Advanced Scientific Instruments Based on Deep Ultraviolet Laser Source (Y31M0112C1), National Key R&D Program of China (2016YFB0700600), and the Key Research Program of Frontier Sciences (QYZDBSSW-SLH024).

■ REFERENCES

(1) Burgert, R.; Schnöckel, H.; Grubisic, A.; Li, X.; Stokes, S. T. Spin Conservation Accounts for Aluminum Cluster Anion Reactivity Pattern with O_2. *Science* **2008**, *319*, 438−442.

(2) Roach, P. J.; Woodward, W. H.; Castleman, A. W., Jr.; Reber, A. C.; Khanna, S. N. Complementary Active Sites Cause Size-Selective Reactivity of Aluminum Cluster Anions with Water. *Science* **2009**, *323*, 492−495.

(3) Luo, Z.; Castleman, A. W., Jr.; Khanna, S. N. Reactivity of Metal Clusters. *Chem. Rev. (Washington, DC, U. S.)* **2016**, *116*, 14456−14492.

(4) Ferrari, P.; Vanbuel, J.; Janssens, E.; Lievens, P. Tuning the Reactivity of Small Metal Clusters by Heteroatom Doping. *Acc. Chem. Res.* **2018**, *51*, 3174−3182.

(5) Knight, W. D. Electronic Shell Structure and Abundance of Sodium Clusters. *Phys. Rev. Lett.* **1984**, *52*, 2141−2143.

(6) Brack, M. The Physics of Simple Metal clusters: Self-Consistent Jellium Model and Semiclassical Approaches. *Rev. Mod. Phys.* **1993**, *65*, 677−732.

(7) De Heer, W. A. The Physics of Simple Metal-Clusters - Experimental Aspects and Simple-Models. *Rev. Mod. Phys.* **1993**, *65*, 611−676.

(8) Luo, Z.; Castleman, A. W., Jr. Special and General Superatoms. *Acc. Chem. Res.* **2014**, *47*, 2931−2940.

(9) Reber, A. C.; Khanna, S. N. Superatoms: Electronic and Geometric Effects on Reactivity. *Acc. Chem. Res.* **2017**, *50*, 255−263.

(10) Jena, P.; Sun, Q. Super Atomic Clusters: Design Rules and Potential for Building Blocks of Materials. *Chem. Rev. (Washington, DC, U. S.)* **2018**, *118*, 5755−5780.

(11) Somorjai, G. A.; Li, Y. *Introduction to Surface Chemistry and Catalysis*, 2nd ed.; Wiley-VCH: Weinheim, Germany, 2011; p 8.

(12) Yin, B.; Luo, Z. Coinage Metal Clusters: From Superatom Chemistry to Genetic Materials. *Coord. Chem. Rev.* **2021**, *429*, 213643.

(13) Gilmour, J. T. A.; Gaston, N. On the Involvement of d-Electrons in Superatomic Shells: the Group 3 and 4 Transition Metals. *Phys. Chem. Chem. Phys.* **2019**, *21*, 8035−8045.

(14) Gilmour, J. T. A.; Gaston, N. 5-Fold Symmetry in Superatomic Scandium Clusters: Exploiting Favourable Orbital Overlap to Sequester Spin. *Phys. Chem. Chem. Phys.* **2020**, *22*, 4051−4058.

(15) Gilmour, J. T. A.; Gaston, N. On the Influence of Exact Exchange on Transition Metal Superatoms. *Phys. Chem. Chem. Phys.* **2020**, *22*, 772−780.

(16) Luo, Z.; Khanna, S. *Metal Clusters and Their Reactivity*; Springer Nature Singapore Pte Ltd., 2020; p 267.

(17) van der Linde, C.; Beyer, M. K. Reactions of $M^+(H_2O)_n$, $n < 40$, M = V, Cr, Mn, Fe, Co, Ni, Cu, and Zn, with D_2O Reveal Water Activation in $Mn^+(H_2O)_n$. *J. Phys. Chem. A* **2012**, *116*, 10676−10682.
(18) van der Linde, C.; Hockendorf, R. F.; Balaj, O. P.; Beyer, M. K. Reactions of Hydrated Singly Charged First-Row Transition-Metal Ions $M^+(H_2O)_n$ (M = V, Cr, Mn, Fe, Co, Ni, Cu, and Zn) toward Nitric Oxide in the Gas Phase. *Chem. - Eur. J.* **2013**, *19*, 3741−3750.
(19) Gernert, I.; Beyer, M. K. Evidence for Electron Transfer in the Reactions of Hydrated Monovalent First-Row Transition-Metal Ions $M(H_2O)_n^+$, M = V, Cr, Mn, Fe, Co, Ni, Cu, and Zn, $n < 40$, toward 1-Iodopropane. *J. Phys. Chem. A* **2017**, *121*, 9557−9566.
(20) Scharfschwerdt, B.; van der Linde, C.; Petru Balaj, O.; Herber, I.; Schütze, D.; Beyer, M. K. Photodissociation and Photochemistry of $V^+(H_2O)_n$, n = 1−4, in the 360−680nm Region. *Low Temp. Phys.* **2012**, *38*, 717−722.
(21) Fox, B. S.; Balteanu, I.; Balaj, O. P.; Liu, H. C.; Beyer, M. K.; Bondybey, V. E. Black Body Radiation Induced Hydrogen Formation in Hydrated Vanadium Cations $V^+(H_2O)_n$. *Phys. Chem. Chem. Phys.* **2002**, *4*, 2224−2228.
(22) Clemmer, D. E.; Chen, Y. M.; Aristov, N.; Armentrout, P. B. Kinetic and Electronic-Energy Dependence of The Reaction of V^+ With D_2O. *J. Phys. Chem.* **1994**, *98*, 7538−7544.
(23) Ma, J.-B.; Zhao, Y.-X.; He, S.-G.; Ding, X.-L. Experimental and Theoretical Study of the Reactions between Vanadium Oxide Cluster Cations and Water. *J. Phys. Chem. A* **2012**, *116*, 2049−2054.
(24) Cheng, P.; Koyanagi, G. K.; Bohme, D. K. Heavy Water Reactions with Atomic Transition-Metal and Main-Group Cations: Gas Phase Room-Temperature Kinetics and Periodicities in Reactivity. *J. Phys. Chem. A* **2007**, *111*, 8561−8573.
(25) Feyel, S.; Schroder, D.; Schwarz, H. Gas-Phase Chemistry of Vanadium Oxide Cluster Cations $V_mO_n^+$ (m = 1−4; n = 1−10) with Water and Molecular Oxygen. *Eur. J. Inorg. Chem.* **2008**, *2008*, 4961−4967.
(26) Su, C. X.; Hales, D. A.; Armentrout, P. B. Collision-Induced Dissociation of V_n^+ (n = 2−20) With Xe - Bond-Energies, Dissociation Pathways, and Structures. *J. Chem. Phys.* **1993**, *99*, 6613−6623.
(27) Fielicke, A.; Kirilyuk, A.; Ratsch, C.; Behler, J.; Scheffler, M.; von Helden, G.; Meijer, G. Structure Determination of Isolated Metal Clusters via Far-Infrared Spectroscopy. *Phys. Rev. Lett.* **2004**, *93*, 023401.
(28) Ratsch, C.; Fielicke, A.; Kirilyuk, A.; Behler, J.; von Helden, G.; Meijer, G.; Scheffler, M. Structure Determination of Small Vanadium Clusters by Density-Functional Theory in Comparison with Experimental Far-Infrared Spectra. *J. Chem. Phys.* **2005**, *122*, 124302.
(29) Xu, J.; Rodgers, M. T.; Griffin, J. B.; Armentrout, P. B. Guided Ion Beam Studies of the Reactions of V_n^+ (n = 2−17) with O_2: Bond Energies and Dissociation Pathways. *J. Chem. Phys.* **1998**, *108*, 9339−9350.
(30) Holmgren, L.; Rosén, A. Vanadium Clusters: Reactivity with CO, NO, O_2, D_2, and N_2. *J. Chem. Phys.* **1999**, *110*, 2629−2636.
(31) Liyanage, R.; Conceicao, J.; Armentrout, P. B. Guided Ion Beam Studies of the Reactions of V_n^+ (n = 2−13) with D_2: Cluster-Deuteride Bond Energies as A Chemical Probe of Cluster Electronic Structure. *J. Chem. Phys.* **2002**, *116*, 936−945.
(32) Feyel, S.; Schroeder, D.; Schwarz, H. Pronounced Cluster-Size Effects: Gas-Phase Reactivity of Bare Vanadium Cluster Cations V_n^+ (n = 1−7) Toward Methanol. *J. Phys. Chem. A* **2009**, *113*, 5625−5632.
(33) Wu, G.; Yang, M.; Guo, X.; Wang, J. Comparative DFT Study of N_2 and NO Adsorption on Vanadium Clusters V_n (n = 2−13). *J. Comput. Chem.* **2012**, *33*, 1854−1861.
(34) Engeser, M.; Weiske, T.; Schroder, D.; Schwarz, H. Oxidative Degradation of Small Cationic Vanadium Clusters by Molecular Oxygen: On the Way from V_n^+ (n = 2−5) to VO_m^+ (m = 1, 2). *J. Phys. Chem. A* **2003**, *107*, 2855−2859.
(35) Hou, G.-L.; Faragó, E.; Buzsáki, D.; Nyulászi, L.; Höltzl, T.; Janssens, E. Observation of the Reaction Intermediates of Methanol Dehydrogenation by Cationic Vanadium Clusters. *Angew. Chem., Int. Ed.* **2021**, DOI: 10.1002/anie.202011109.
(36) Langeslay, R. R.; Kaphan, D. M.; Marshall, C. L.; Stair, P. C.; Sattelberger, A. P.; Delferro, M. Catalytic Applications of Vanadium: A Mechanistic Perspective. *Chem. Rev. (Washington, DC, U. S.)* **2019**, *119*, 2128−2191.
(37) Whittingham, M. S. Lithium Batteries and Cathode Materials. *Chem. Rev. (Washington, DC, U. S.)* **2004**, *104*, 4271−4302.
(38) Krusin-Elbaum, L.; Newns, D. M.; Zeng, H.; Derycke, V.; Sun, J. Z.; Sandstrom, R. Room-Temperature Ferromagnetic Nanotubes Controlled by Electron or Hole Doping. *Nature* **2004**, *431*, 672−676.
(39) Zhang, M. Q.; Zhao, Y. X.; Liu, Q. Y.; Li, X. N.; He, S. G. Does Each Atom Count in the Reactivity of Vanadia Nanoclusters? *J. Am. Chem. Soc.* **2017**, *139*, 342−347.
(40) Meza, B.; Miranda, P.; Castro, M. Structural and Electronic Properties of Hydrated V_nH_2O and $V_n^+H_2O$, $n \leq 13$, Systems. *J. Phys. Chem. C* **2017**, *121*, 4635−4649.
(41) Zhang, H.; Wu, H.; Jia, Y.; Yin, B.; Geng, L.; Luo, Z.; Hansen, K. Hydrogen Release From a Single Water Molecule on V_n^+ ($3 \leq n \leq 30$). *Commun. Chem.* **2020**, *3*, 148.
(42) Geng, L.; Weng, M.; Xu, C.-Q.; Zhang, H.; Cui, C.; Wu, H.; Chen, X.; Hu, M.; Lin, H.; Sun, Z.-D.; et al. $Co_{13}O_8$—Metal-loxocubes: A New Class of Perovskite-Like Neutral Clusters with Cubic Aromaticity. *Natl. Sci. Rev.* **2021**, *8*, nwaa201.
(43) Wu, H.; Yuan, C.; Zhang, H.; Yang, G.; Cui, C.; Yang, M.; Bian, W.; Fu, H.; Luo, Z.; Yao, J. Ultrafast Deep-Ultraviolet Laser Ionization Mass Spectrometry Applicable To Identify Phenylenediamine Isomers. *Anal. Chem.* **2018**, *90*, 10635−10640.
(44) Zhang, H.; Wu, H.; Jia, Y.; Geng, L.; Luo, Z.; Fu, H.; Yao, J. An Integrated Instrument of DUV-IR Photoionization Mass Spectrometry and Spectroscopy for Neutral Clusters. *Rev. Sci. Instrum.* **2019**, *90*, 073101.
(45) Luo, Z. X.; Smith, J. C.; Woodward, W. H.; Castleman, A. W., Jr. Reactivity of Aluminum Clusters with Water and Alcohols: Competition and Catalysis? *J. Phys. Chem. Lett.* **2012**, *3*, 3818−3821.
(46) Du, Y.; Sheng, H.; Astruc, D.; Zhu, M. Atomically Precise Noble Metal Nanoclusters as Efficient Catalysts: A Bridge between Structure and Properties. *Chem. Rev.* **2020**, *120*, 526−622.
(47) Oganov, A. R.; Glass, C. W. Crystal Structure Prediction Using Ab Initio Evolutionary Techniques: Principles and Applications. *J. Chem. Phys.* **2006**, *124*, 244704.
(48) Kresse, G.; Furthmüller, J. Efficient Iterative Schemes for Ab Initio Total-Energy Calculations Using a Plane-Wave Basis Set. *Phys. Rev. B: Condens. Matter Mater. Phys.* **1996**, *54*, 11169−11186.
(49) Becke, A. D. Density-Functional Exchange-Energy Approximation with Correct Asymptotic Behavior. *Phys. Rev. A: At., Mol., Opt. Phys.* **1988**, *38*, 3098−3100.
(50) Perdew, J. P.; Wang, Y. Accurate and Simple Analytic Representation of the Electron-Gas Correlation Energy. *Phys. Rev. B: Condens. Matter Mater. Phys.* **1992**, *45*, 13244−13249.
(51) Schäfer, A.; Huber, C.; Ahlrichs, R. Fully Optimized Contracted Gaussian Basis Sets of Triple Zeta Valence Quality for Atoms Li to Kr. *J. Chem. Phys.* **1994**, *100*, 5829−5835.
(52) Frisch, M. J.; Trucks, G. W.; Schlegel, H. B.; Scuseria, G. E.; Robb, M. A.; Cheeseman, J. R.; Scalmani, G.; Barone, V.; Mennucci, B.; Petersson, G. A.; et al. *Gaussian 09*, Rev. E.01; Wallingford, CT, 2009.
(53) Zhao, J.; Huang, X.; Jin, P.; Chen, Z. Magnetic Properties of Atomic Clusters and Endohedral Metallofullerenes. *Coord. Chem. Rev.* **2015**, *289−290*, 315−340.
(54) Douglass, D. C.; Bucher, J. P.; Bloomfield, L. A. Magnetic Studies of Free Nonferromagnetic Clusters. *Phys. Rev. B: Condens. Matter Mater. Phys.* **1992**, *45*, 6341−6344.
(55) Alonso, J. A. Electronic and Atomic Structure, and Magnetism of Transition-Metal Clusters. *Chem. Rev. (Washington, DC, U. S.)* **2000**, *100*, 637−678.
(56) Taneda, A.; Shimizu, T.; Kawazoe, Y. Stable Disordered Structures of Vanadium Clusters. *J. Phys.: Condens. Matter* **2001**, *13*, L305−L312.

(57) Cox, D. M.; Whetten, R. L.; Zakin, M. R.; Trevor, D. J.; Reichmann, K. C.; Kaldor, A. Ionization Threshold Energies for Metal Clusters. *AIP Conf. Proc.* **1986**, *146*, 527−530.
(58) Becke, A. D. Density-Functional Thermochemistry. III. The Role of Exact Exchange. *J. Chem. Phys.* **1993**, *98*, 5648−5652.
(59) Lee, C.; Yang, W.; Parr, R. G. Development of the Colle-Salvetti Correlation-Energy Formula into a Functional of the Electron Density. *Phys. Rev. B: Condens. Matter Mater. Phys.* **1988**, *37*, 785−789.
(60) Wang, H. Q.; Li, H. F.; Kuang, X. Y. Probing the Structural and Electronic Properties of Small Vanadium Monoxide Clusters. *Phys. Chem. Chem. Phys.* **2012**, *14*, 5272−5283.

https://dx.doi.org/10.1021/acs.jpclett.0c03809
J. Phys. Chem. Lett. 2021, 12, 1593−1600